Influence of Ski Bending Stiffness on the Turning Radius of Alpine Skis at Different Edging Angles and Velocities

Dieter Heinrich[1], Martin Mössner[1], Peter Kaps[2], Herwig Schretter[3], and Werner Nachbauer[1]

[1] University of Innsbruck, Department of Sports Science, dieter.heinrich@uibk.ac.at
[2] University of Innsbruck, Department of Engineering Mathematics, Geometry and Computer Science
[3] HTM Tyrolia, Schwechat, Austria

Abstract. Carved turns with Alpine Skis were investigated using a computer simulation model. Varied input data to the model were the bending stiffness of the skis, the edging angle, and the velocity. Results include the turn radius and the force distribution along the running surface of the skis.

1 Introduction

In Alpine skiing turns of a skier depend on several factors: 1) ski properties like bending stiffness, torsional stiffness or side geometry, 2) actions of the skier like edging, loading or unloading a ski, 3) snow properties, and 4) velocity.

Although there are a number of publications concerning skiing in general (i.e. Howe 1983, Lind and Sanders 1996) and simulation in skiing (i.e. Renshaw and Mote 1991, Casolo et al. 1997, Tada and Hirano 1999, Nordt et al. 1999, Kaps et al. 2001, Bruck et al. 2003, Federolf 2005) there is a lack of quantitative studies concerning the influence of different factors on the turn of a skier.

The aim of the present paper was to study the influence of the bending stiffness on the turn radius of a carved turn by means of an improved implementation of a computer simulation model for a ski sledge (Bruck et al. 2003, Mössner et al. 2006). Input data of the simulation model are data of ski properties as well as snow properties. Data of ski properties include side geometry, bending stiffness, torsional stiffness and damping. Data of snow properties include compressibility of snow, ultimate shear pressure (limit where snow starts to shear), and coefficient of friction between snow and skis. By means of this simulation model three distributions of the bending stiffness of a carving ski were investigated at three different edging angles and two initial velocities. Results include the turn radius of the sledge and the force distribution along the running surface of the ski. In the next section the simulation model is explained. After that varied input data to the model are described. Finally simulation results are presented and discussed.

2 Method

2.1 Model Description

Fig. 1: Model of a sledge on two skis implemented in the multi-body simulation software LMS Virtual.Lab.

The Ski and the Sledge. For the investigations a carving ski with nominal length of 170 cm and a side cut radius r_s = 12.5 m was used. The ski was modeled as a multi-body system. The body of the ski was divided into 19 segments along its longitudinal axis. Adjacent segments were connected by two revolute joints in order to model bending and torsion of the ski. Stiffness and damping properties of the ski were represented by spring damper elements integrated in the revolute joints.

As a simple model of the skier a sledge was used. The sledge consisted of a rigid frame where the edging angle of the skis could be fixed at user defined values. The mass of the sledge was about 75 kg comparable to the mass of an average skier. The sledge and the skis were rigidly connected. For the dynamic simulation of the movement, the ski sledge was implemented in the multi-body system software LMS Virtual.Lab (Fig.1).

C**ontact between Ski and Snow**. In order to model the contact between the skis and the snow three types of forces were used: penetration force, shear force and kinetic friction force. For a precise description of the contact between the skis and the snow, ski segments were further divided into sub-segments. The penetration force was determined using a hypoplastic force-penetration relationship. This relationship was considered in order to describe the local loading and unloading behavior of snow. The snow was locally loaded as long as the penetration depths of the frontal parts of the ski were less than the actual penetration depth. In this situation the penetration force was calculated according to Eq.1, where H means the snow hardness, L the length of the sub-segment, e the penetration depth of the edge, θ the edging angle of the ski, and V the snow volume which was displaced by a sub-segment.

$$F_p = \frac{H \cdot L \cdot e^2}{2 \cdot \tan(\theta)} = H \cdot V \tag{1}$$

On the other hand, if the penetration depth of any frontal part was larger than the actual penetration depth it was assumed that the actual part of the ski just follows the track, dug into the snow. Thus unloading was assumed and ideally no penetration force was applied. Shear force was modeled based on metal cutting theory (Shaw 1984). Knowing the ultimate shear pressure p^* of snow, the reaction force on a sub-segment was calculated using:

$$F_s = p^* \cdot e \cdot L \tag{2}$$

Friction between the ski and the snow was modeled using Coulomb friction and a friction coefficient $\mu = 0.07$ (Kaps et al. 1996):

$$F_f = \mu \cdot F_p \tag{3}$$

Details concerning the implementation of the contact between ski and snow are described in Mössner et al. (2006).

2.2 Simulations with Varied Bending Stiffness

Dynamic simulations of the movement of the ski sledge were carried out using three different distributions of the bending stiffness of the carving skis: the real distribution, a soft distribution and a stiff distribution (Fig.2). The real distribution of the bending stiffness was determined in a bending experiment. The soft distribution of the bending stiffness was set to 50 % of the real distribution of the ski. The stiff distribution of the bending stiffness was set to 200 % of the real distribution of the ski.

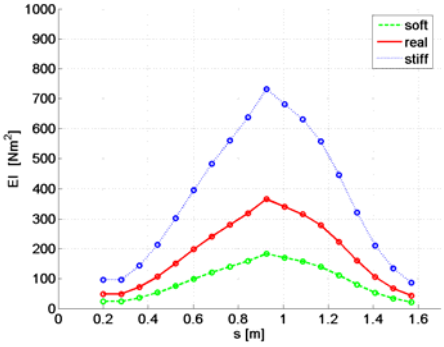

Fig. 2: Distribution of the bending stiffness *EI* of the soft, real and stiff ski.

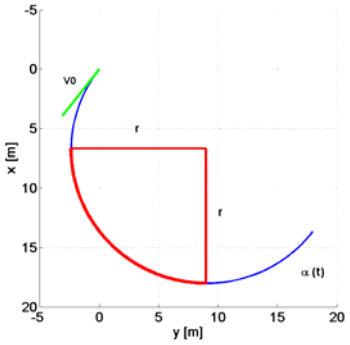

Fig. 3: Track of the sledge α(t), average turn radius *r*, and initial velocity v_0.

Using each of these three configurations, dynamic simulations of a single turn of the ski sledge were computed (the start position of the ski sledge was fixed at an angle $\phi = 39°$ between the longitudinal axis of the skis and the fall line of the slope). In the simulations two different initial velocities of $v_0 = 1$ and 5 *m/s* and three constant edging angles of $\theta = 15°, 35°,$ and $55°$ were used. Other parameters such as torsional stiffness, damping properties and side geometry of the skis or snow properties were kept constant in order to study the effects solely due to the different configurations.

After the simulations an average turn radius of the sledge was calculated fitting the track data of the sledge to a least square approximation of a quarter circle. An average turn radius was chosen to get a criterion to compare the simulations. To give reasons for the resulted turn radii the force distribution along the running surface of the ski and the bending deformation of the side edge of the skis were studied.

3 Results and Discussion

The simulations with the soft, real and stiff skis showed that a larger edging angle resulted in a smaller turn radius (Tab. 1). The two main reasons for a smaller turn radius were: increased bending deformation of the skis and less skidding of the skis. At an edged and unloaded ski only a small part of the shovel and a small part of the tail of the ski are in contact with the snow surface. Loading the ski, the ski bends until the whole edge of the ski contacts the snow surface. At an increased edging angle it's geometrically obvious that the ski has to bend more until its edge contacts the snow surface (the requirement that the loading is sufficient to bend the ski until it contacts the snow surface is usually fulfilled).

Ski type	θ	r_1	r_5	r_{H0}	r_{H4}
Soft	15	16.32	22.21	12.07	11.51
Real	15	15.85	23.79	12.07	11.51
Stiff	15	17.61	29.44	12.07	11.51
Soft	35	11.77	13.14	10.24	9.25
Real	35	11.33	12.69	10.24	9.25
Stiff	35	11.67	13.06	10.24	9.25
Soft	55	7.74	8.34	7.17	6.22
Real	55	7.78	8.05	7.17	6.22
Stiff	55	9.06	9.23	7.17	6.22

Tab. 1: Average turn radius r_1 , r_5 *[m]* of the soft, real and stiff skis at edging angles of $\theta = 15°, 35°,$ and $55°$ and initial velocities $v_0 = 1$ *m/s* (r_1) and *5 m/s* (r_5) and turn radius according to Howe (1983) r_{H0} , r_{H4} *[m]* with penetration depths of zero (r_{H0}) and *4 mm* (r_{H4}).

If a ski with a side cut radius r_s and an edging angle θ is pressed on a rigid surface until the edge has full contact, the edge assumes the form of a circular arc with a radius $r_H = r_s \cdot \cos(\theta)$. On a non rigid surface this radius is further decreased with increasing penetration depth (Howe 1983). Assuming that the ski follows its deformed edge and no skidding occurs the turn radius is equal to r_H. Less skidding happened because at equal load and a higher edging angle the penetration depth of the ski increased (Eq.1). Hence, the shear force increased (Eq.2). Increased shear force led to increased side guidance and hence skidding decreased. Comparing the turn radius r_H and the average turn radius the amount of skidding at each edging angle could be quantified.

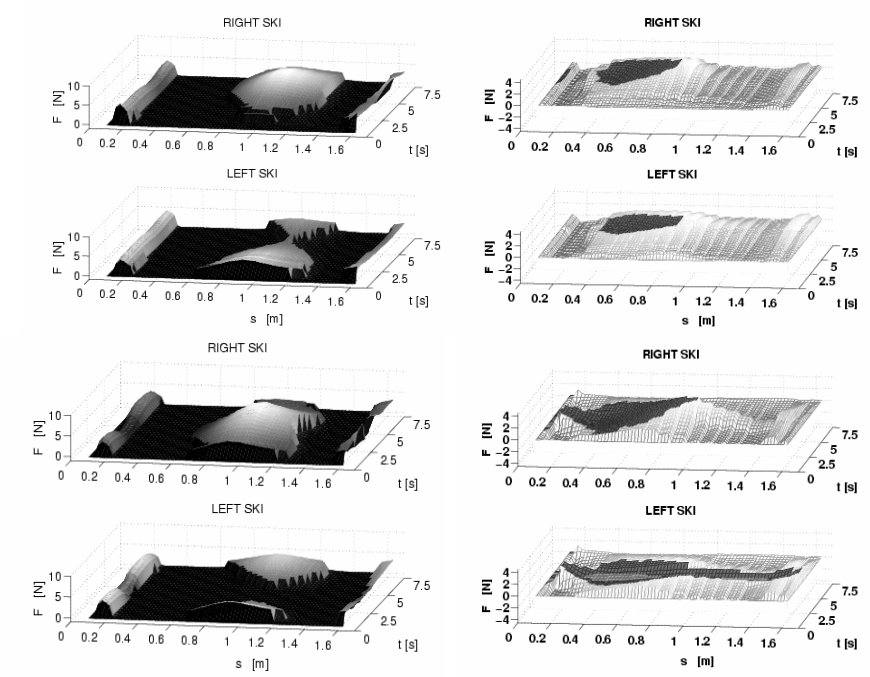

Fig. 4: Force distribution along the running surface of the real skis normal to snow surface (left) and parallel to the snow surface (right). Results of a single turn to the left (t = 0 …7.5s) at a constant edging angle $\theta = 35°$ and initial velocities $v_0 = 1$ *m/s* (above) and $v_0 = 5$ *m/s* (below) are shown. The tip of the ski is located at s = 0. The force distribution normal to the snow surface resulted due the loading – unloading behaviour of snow. Dark regions at the force distribution parallel to the snow surface in the right figure indicated the regions where the ultimate shear pressure of snow was reached and skidding was dominant.

The simulations with the soft, real and stiff skis showed that raising the initial velocity from $v_0 = 1$ to 5 *m/s* resulted in a larger turn radius. The larger turn radius was a consequence of the increased centrifugal force. Consequently, because the centrifugal force is directed radially, the lateral load on the skis increased and skidding became more dominant, especially at low edging angles.

Comparing the simulations at an initial velocity of $v_0 = 1$ *m/s* showed that at edging angles of $\theta = 15°$ and $35°$ the turn radius of the real ski was smallest whereas at an edging angle of $\theta = 55°$ the turn radius of the soft ski was smallest. In order to achieve a small turn two requirements have to be fulfilled: 1) little skidding which is a consequence of the force distribution along the running surface of the skis (Eq.1 and Eq.2) and 2) high bending deformation of the skis. The highest bending deformation was always present at the soft skis (lowest bending stiffness). However, at edging angles of $\theta = 15°$ and $35°$ skidding at the soft skis was more dominant than at the real skis and as a consequence a larger turn radius resulted. In Fig. 4 the force distribution along the running surface of the real skis and an edging angle of $\theta = 35°$ is presented.

Comparing the simulations at an initial velocity of $v_0 = 5$ *m/s* showed that at an edging angle of $\theta = 15°$ the turn radius of the soft ski was smallest whereas at edging angles of $\theta = 35°$ and $55°$ the turn radius of the real ski was smallest. The results at the edging angle of $\theta = 15°$ have to be considered carefully, because during the simulations with the real and the stiff skis the inner ski of the sledge lifted from the snow surface. Consequently the whole lateral load was shifted to the outer ski and skidding became dominant. At edging angles of $\theta = 35°$ and $55°$ the bending stiffness of real ski resulted in the best combination of bending deformation and skidding. In Fig. 4 the force distribution along the running surface of the real skis and an edging angle of $\theta = 35°$ is presented.

Acknowledgement

The investigation was supported by HTM Tyrolia.

References

Bruck, F., Lugner, P., and Schretter, H. (2003). A Dynamic Model for the Performance of Carving Skis, Skiing Trauma and Safety, 14th vol., ASTM STP 1440 (West Conshohocken, US-PA) (R.J. Johnson, M.K. Lamont, and J.E. Shealy, eds.), 10-23.

Casolo, F., Lorenzi, V., Vallatta, and A., Zappa, B. (1997). Simulation Techniques Applied to Skiing Mechanics, Science and Skiing (London, UK) (E. Müller, H. Schwameder, E. Kornexl, and C. Raschner eds.), 116-130.

Federolf, P.A. (2005). Finite Element Simulation of a Carving Snow Ski, Ph.D. thesis, Swiss Fed. Inst. of Tech., Zurich, CH.

Howe, J. (1983). Skiing Mechanics, Poudre Press, Laporte, US-CO.

Kaps, P., Nachbauer, W., and Mössner, M. (1996). Determination of Kinetic Friction and Drag Area in Alpine Skiing, Skiing Trauma and Safety, 10th vol., ASTM STP 1266 (Philadelphia, US-PA) (C.D. Mote, R.J. Johnson, W. Hauser, and P.S. Schaff, eds.), 165-177.

Kaps, P., Mössner, M., Nachbauer, W., and Stenberg, R. (2001). Pressure Distribution Under a Ski During Carved Turns, Science and Skiing II (Hamburg, DE) (E. Müller, H. Schwameder, C. Raschner, S. Lindiger, and E. Kornexl, eds.), 180-202.

Lind, D. and Sanders, S.P. (1996). The Physics of Skiing, Springer, New York, US-NY.

Mössner, M., Heinrich, D., Schindelwig K., Kaps, P., Lugner, P., Schmiedmayer H.B., Schretter, H., and Nachbauer, W. (2006). Modeling of the Ski-Snow Contact for a Carved Turn. The Engineering of Sport 6, 2nd vol. (Munich, DE) (E.F. Moritz and S.J. Haake, eds.), International Sports Engineering Association (ISEA), 2006, 195-200.

Nordt, A.A., Springer, G.S., and Kollár, L.P. (1999). Computing the Mechanical Properties of Alpine Skis, Sports Engineering 2, 65-84.

Renshaw, A.A. and Mote, C.D. (1991). A Model for the Turning Snow Ski, Skiing Trauma and Safety, 8th vol., ASTM STP 1104 (Philadelphia, US-PA) (C.D. Mote and R.J. Johnson, eds.), 217-238.

Shaw, M.C. (1984). Metal Cutting Principles, Oxford Univ. Press, Oxford, GB.

Tada, N. and Hirano, Y. (1999). Simulation of a Turning Ski Using Ice Cutting Data, Sports Engineering 2, 55-64.